NATIONAL ENERGY TECHNOLOGY LABORATORY

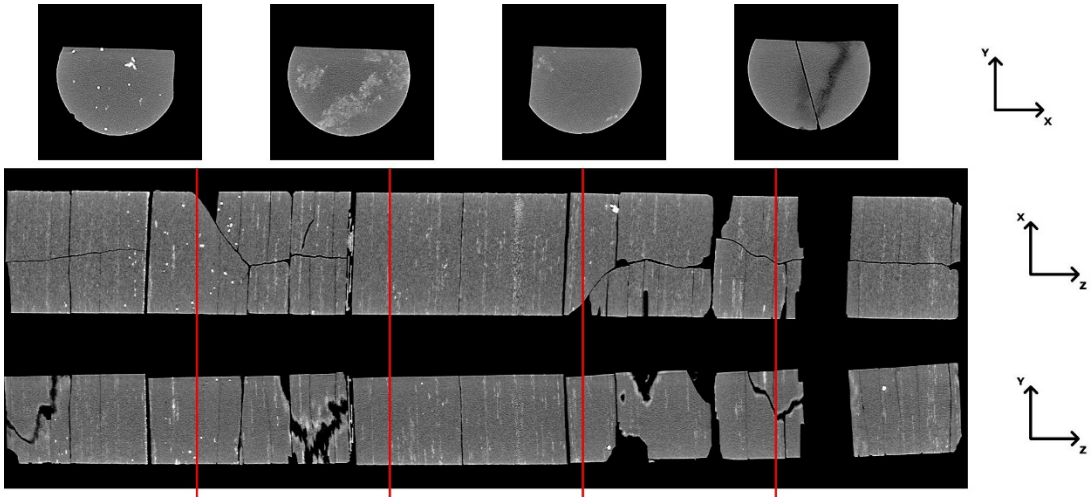

CT Scanning and Geophysical Measurements of the Marcellus Formation from the Tippens 6HS Well

15 February 2018

U.S. DEPARTMENT OF ENERGY | NATIONAL ENERGY TECHNOLOGY LABORATORY

Office of Fossil Energy

NETL-TRS-3-2018

Disclaimer

Cover Illustration: Computed tomography scans a section of the Tippens 6HS well from 5613–5316 ft, in the three primary orthogonal directions.

Suggested Citation: Crandall, D.; Paronish, T.; Brown, S.; Martin, K.; Moore, J.; Carr, T. R.; Panetta, B. *CT Scanning and Geophysical Measurements of the Marcellus Formation from the Tippens 6HS Well;* NETL-TRS-3-2018; NETL Technical Report Series; U.S. Department of Energy, National Energy Technology Laboratory: Morgantown, WV, 2018; p 32.

An electronic version of this report can be found at:

http://netl.doe.gov/research/on-site-research/publications/featured-technical-reports

https://edx.netl.doe.gov/ucr

The data in this report can be accessed from NETL's Energy Data eXchange (EDX) online system using the following link: https://edx.netl.doe.gov/dataset/tippens-6hs-well

CT Scanning and Geophysical Measurements of the Marcellus Formation from the Tippens 6HS Well

Dustin Crandall[1], Thomas Paronish[2,3], Sarah Brown[4], Keithan Martin[2,3], Johnathan Moore[4], Timothy R. Carr[3], and Brian Panetta[5]

[1] U.S. Department of Energy, Office of Research and Development, National Energy Technology Laboratory, 3610 Collins Ferry Road, Morgantown, WV 26507

[2] U.S. Department of Energy, National Energy Technology Laboratory, ORAU, 3610 Collins Ferry Road, Morgantown, WV 26507

[3] Department of Geology and Geography, West Virginia University, 98 Beechurst Avenue, Morgantown, WV 26506

[4] U.S. Department of Energy, National Energy Technology Laboratory, AECOM, 3610 Collins Ferry Road, Morgantown, WV 26507

[5]Eclipse Resources, 2121 Old Gatesburg Road, Suite 110, State College, PA 16803

NETL-TRS-3-2018

15 February 2018

NETL Contacts:

Dustin Crandall, Principal Investigator

J. Alexandra Hakala, Technical Portfolio Lead

David Alman, Executive Director, Acting, Research & Innovation Center

This page intentionally left blank.

Table of Contents

List of Figures

List of Tables

Acronyms, Abbreviations, and Symbols

Term	Description
2D	Two-dimensional
3D	Three-dimensional
CT	Computed tomography
EDX	NETL's Energy Data eXchange
MSCL	Multi-Sensor Core Logger
NETL	National Energy Technology Laboratory
WVU	West Virginia University
XRF	X-ray fluorescence

Acknowledgments

This work was completed at the National Energy Technology Laboratory (NETL) with support from U.S. Department of Energy's (DOE) Office of Fossil Energy Oil & Gas Program. The authors wish to acknowledge Alexandra Hakala (NETL Research and Innovation Center), Jared Ciferno (NETL Technology Development and Integration Center) and Elena Melchert (DOE Office of Fossil Energy) for programmatic guidance, direction, and support.

The authors would like to thank Bryan Tennant, Karl Jarvis, Scott Workman, and Roger Lapeer for data collection and technical support. Thank you to Eclipse Resources for allowing us to work with this core. Thank you to Kelly Rose, Dustin McIntyre and Mark McKoy for laboratory support. This research was supported in part by appointments from the NETL Research Participation Program, sponsored by the U.S. DOE and administered by the Oak Ridge Institute for Science and Education.

ABSTRACT

The computed tomography (CT) facilities and the Multi-Sensor Core Logger (MSCL) at the National Energy Technology Laboratory (NETL) Morgantown, West Virginia site were used to characterize core of the Marcellus Shale from a vertical well drilled in Eastern Ohio. The core is from the Tippens 6HS Well in Monroe County, Ohio and is comprised primarily of the Marcellus Shale from depths of 5550 to 5663 ft.

The primary impetus of this work is a collaboration between West Virginia University (WVU) and NETL to characterize core from multiple wells to better understand the structure and variation of the Marcellus and Utica shale formations. As part of this effort, bulk scans of core were obtained from the Tippens 6HS Well, provided by Eclipse Resources. This report, and the associated core scans, provide detailed datasets not typically available from unconventional shales for analysis. The datasets are presented in this report, and can be accessed from NETL's Energy Data eXchange (EDX) online system using the following link: https://edx.netl.doe.gov/dataset/tippens-6hs-well.

All equipment and techniques used were non-destructive, enabling future examinations to be performed on these cores. None of the equipment used was suitable for direct visualization of the shale pore space, although fractures and discontinuities were detectable with the methods tested. Low resolution CT imagery with the NETL medical CT scanner was performed on the entire core. Qualitative analysis of the medical CT images, coupled with x-ray fluorescence (XRF) and magnetic susceptibility measurements from the MSCL were useful in identifying zones of interest for more detailed analysis as well as fractured zones. The ability to quickly identify key areas for more detailed study with higher resolution will save time and resources in future studies. The combination of methods used provided a multi-scale analysis of this core and provides both a macro and micro description of the core that is relevant for many subsurface energy-related examinations that have traditionally been performed at NETL.

1. INTRODUCTION

Evaluation of reservoir samples can support resource estimation and choice of effective extraction methodology. While it is common for commercial entities to perform these characterizations, the resources necessary to conduct these analyses are not always available to the broader interest base, such as state agencies and research-based consortiums. To meet the growing need for comprehensive and high quality lithologic data for research initiatives, the National Energy Technology Laboratory (NETL) has used available resources in conjunction with previous techniques and new, innovative methodologies to develop a systematic approach for the evaluation of cores. In this report, data collected from a Marcellus Shale production well in Monroe County, Ohio are presented as one part of a broader collaborative effort by West Virginia University (WVU) and NETL to better characterize this important spatially heterogeneous formation.

In this study, the primary objective was to characterize core from depth with methods not available to most researchers. The data is presented in several formats (here and online) that are potentially useful for various analyses, but little detailed analysis is presented in this report as the research objective was not to do a site characterization, but rather to develop the data for others to utilize and to create a digital representation of the core that could be preserved.

The core is from the Tippens 6HS well (API 34-111-24358), drilled in Monroe County, Ohio (39.678551 N, 81.025461 W). The Tippens 6HS well has a single core stored in 38 boxes and covers a depth of 5555–5663 ft. As shown in Figures 1 and 2 (shapefiles from EIA, 2018), Monroe County is on the eastern edge of Ohio, bordering West Virginia; Marcellus shale in this area is between a depth of 5000–6000 ft and has an average thickness of 50–100 ft.

Field name	IGSN	Link
Tippens 6HS, Core 1, Box 1/38	IENTL00QV	https://app.geosamples.org/sample/igsn/IENTL00QV
Tippens 6HS, Core 1, Box 2/38	IENTL00QW	https://app.geosamples.org/sample/igsn/IENTL00RO
Tippens 6HS, Core 1, Box 3/38	IENTL00QX	https://app.geosamples.org/sample/igsn/IENTL00QX
Tippens 6HS, Core 1, Box 4/38	IENTL00QY	https://app.geosamples.org/sample/igsn/IENTL00QY
Tippens 6HS, Core 1, Box 5/38	IENTL00QZ	https://app.geosamples.org/sample/igsn/IENTL00QZ
Tippens 6HS, Core 1, Box 6/38	IENTL00R0	https://app.geosamples.org/sample/igsn/IENTL00R0
Tippens 6HS, Core 1, Box 7/38	IENTL00R1	https://app.geosamples.org/sample/igsn/IENTL00R1
Tippens 6HS, Core 1, Box 8/38	IENTL00R2	https://app.geosamples.org/sample/igsn/IENTL00R2
Tippens 6HS, Core 1, Box 9/38	IENTL00R3	https://app.geosamples.org/sample/igsn/IENTL00R3
Tippens 6HS, Core 1, Box 10/38	IENTL00R4	https://app.geosamples.org/sample/igsn/IENTL00R4
Tippens 6HS, Core 1, Box 11/38	IENTL00R5	https://app.geosamples.org/sample/igsn/IENTL00R5
Tippens 6HS, Core 1, Box 12/38	IENTL00R6	https://app.geosamples.org/sample/igsn/IENTL00R6
Tippens 6HS, Core 1, Box 13/38	IENTL00R7	https://app.geosamples.org/sample/igsn/IENTL00R7
Tippens 6HS, Core 1, Box 14/38	IENTL00R8	https://app.geosamples.org/sample/igsn/IENTL00R8
Tippens 6HS, Core 1, Box 15/38	IENTL00R9	https://app.geosamples.org/sample/igsn/IENTL00R9
Tippens 6HS, Core 1, Box 16/38	IENTL00RA	https://app.geosamples.org/sample/igsn/IENTL00RA
Tippens 6HS, Core 1, Box 17/38	IENTL00RB	https://app.geosamples.org/sample/igsn/IENTL00RB
Tippens 6HS, Core 1, Box 18/38	IENTL00RC	https://app.geosamples.org/sample/igsn/IENTL00RC
Tippens 6HS, Core 1, Box 19/38	IENTL00QU	https://app.geosamples.org/sample/igsn/IENTL00QU
Tippens 6HS, Core 1, Box 20/38	IENTL00RD	https://app.geosamples.org/sample/igsn/IENTL00RD
Tippens 6HS, Core 1, Box 21/38	IENTL00RE	https://app.geosamples.org/sample/igsn/IENTL00RE
Tippens 6HS, Core 1, Box 22/38	IENTL00RF	https://app.geosamples.org/sample/igsn/IENTL00RF
Tippens 6HS, Core 1, Box 23/38	IENTL00RG	https://app.geosamples.org/sample/igsn/IENTL00RG

Tippens 6HS, Core 1, Box 24/38	IENTL00RH	https://app.geosamples.org/sample/igsn/IENTL00RH
Tippens 6HS, Core 1, Box 25/38	IENTL00RI	https://app.geosamples.org/sample/igsn/IENTL00RI
Tippens 6HS, Core 1, Box 26/38	IENTL00RJ	https://app.geosamples.org/sample/igsn/IENTL00RJ
Tippens 6HS, Core 1, Box 27/38	IENTL00RK	https://app.geosamples.org/sample/igsn/IENTL00RK
Tippens 6HS, Core 1, Box 28/38	IENTL00RL	https://app.geosamples.org/sample/igsn/IENTL00RL
Tippens 6HS, Core 1, Box 29/38	IENTL00RM	https://app.geosamples.org/sample/igsn/IENTL00RM
Tippens 6HS, Core 1, Box 30/38	IENTL00RN	https://app.geosamples.org/sample/igsn/IENTL00RN
Tippens 6HS, Core 1, Box 31/38	IENTL00RO	https://app.geosamples.org/sample/igsn/IENTL00RO
Tippens 6HS, Core 1, Box 32/38	IENTL00RP	https://app.geosamples.org/sample/igsn/IENTL00RP
Tippens 6HS, Core 1, Box 33/38	IENTL00RQ	https://app.geosamples.org/sample/igsn/IENTL00RQ
Tippens 6HS, Core 1, Box 34/38	IENTL00RR	https://app.geosamples.org/sample/igsn/IENTL00RR
Tippens 6HS, Core 1, Box 35/38	IENTL00RS	https://app.geosamples.org/sample/igsn/IENTL00RS
Tippens 6HS, Core 1, Box 36/38	IENTL00RT	https://app.geosamples.org/sample/igsn/IENTL00RT
Tippens 6HS, Core 1, Box 37/38	IENTL00RU	https://app.geosamples.org/sample/igsn/IENTL00RU
Tippens 6HS, Core 1, Box 38/38	IENTL00RV	https://app.geosamples.org/sample/igsn/IENTL00RV

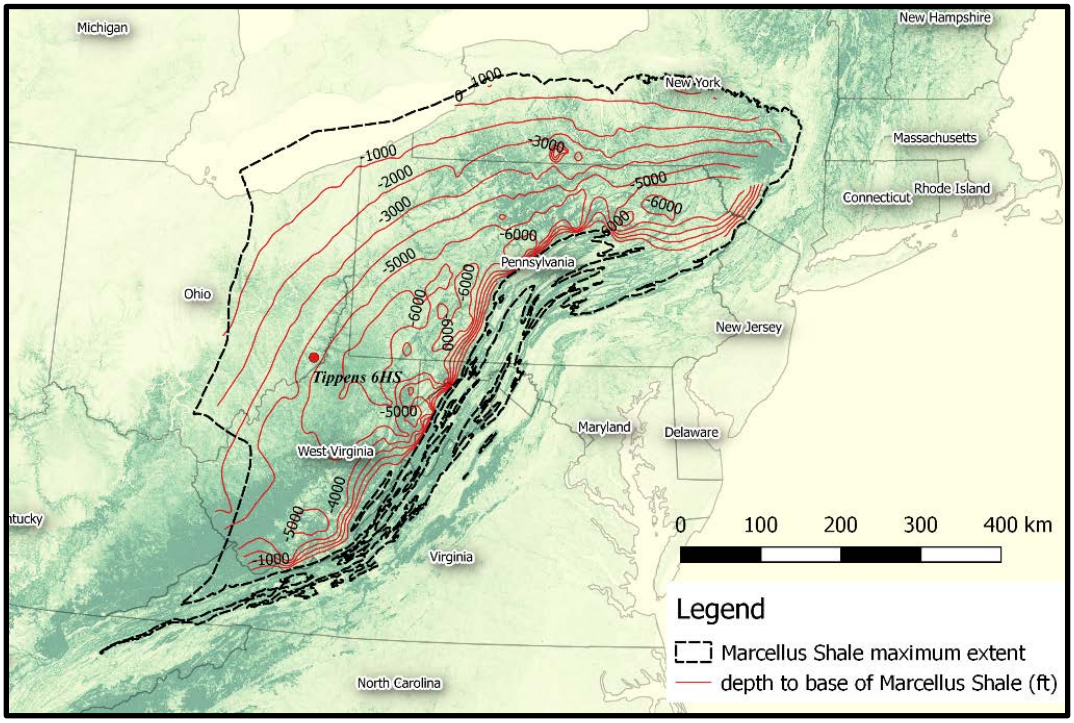

Figure 1: Depth to the Marcellus Shale base. Data files from EIA, 2018.

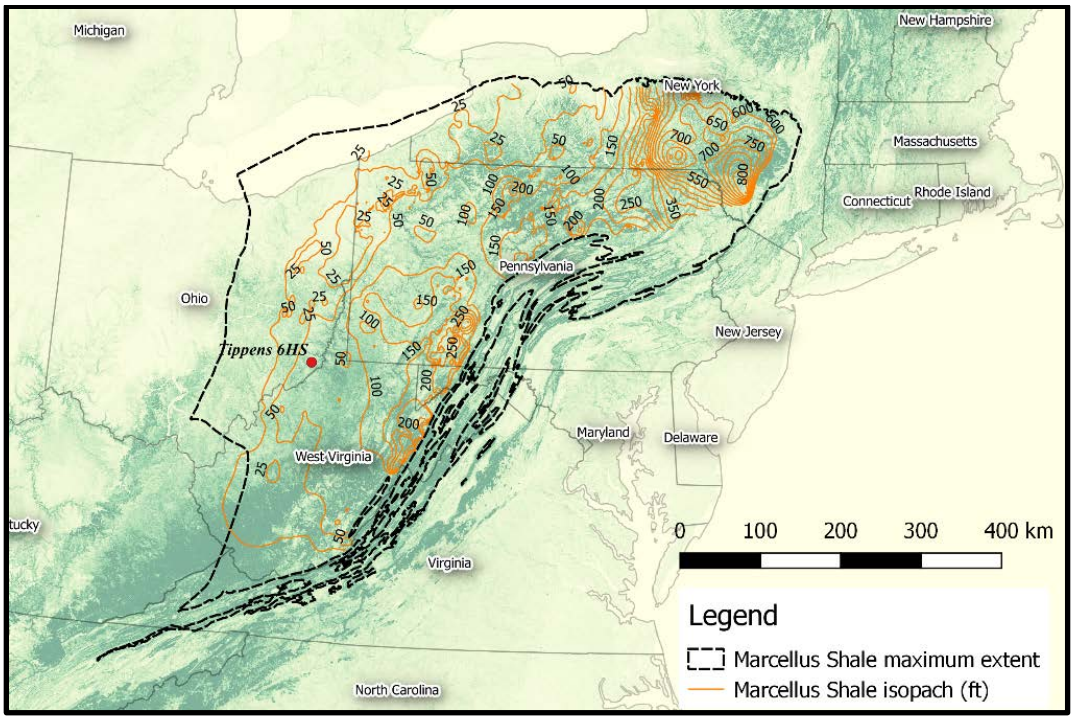

Figure 2: Marcellus Shale thickness. Data files from EIA, 2018.

2. CORE DESCRIPTION

The core contains fine grain organic-rich shale interbedded with fossiliferous calcareous shale and lighter silty mudstone (silty shale). Fine to medium silt-sized quartz and mica are present with minor calcite cement and extensive pyrite formation and replacement. The drilling was perpendicular to bedding, many of the thin beds (0.1 to 0.5 cm thick) in the fine-grained mudstone are now highlighted as fracture surfaces, some filled with pyrite. Most fractures are parallel to the beds, but there are several sections with near vertical fractures. Some bedding planes are disrupted and appear to be relict storm surfaces with rip-up clasts, while others are undulating. At a depth of 5577 ft, the bedding transitions from thinly laminar to massively bedded. The majority of the nodules and concretions are either wholly pyrite or consist of a combination of calcite and pyrite. Some nodules are well rounded (5594.5 ft) while others are bulbous and contorted and may be the result of replacement and infilling of bioturbation structures (5591.8 ft).

2.1 CORE PHOTOGRAPHS

The following figures are photographs of the 1/3 slabbed core, as received at NETL.

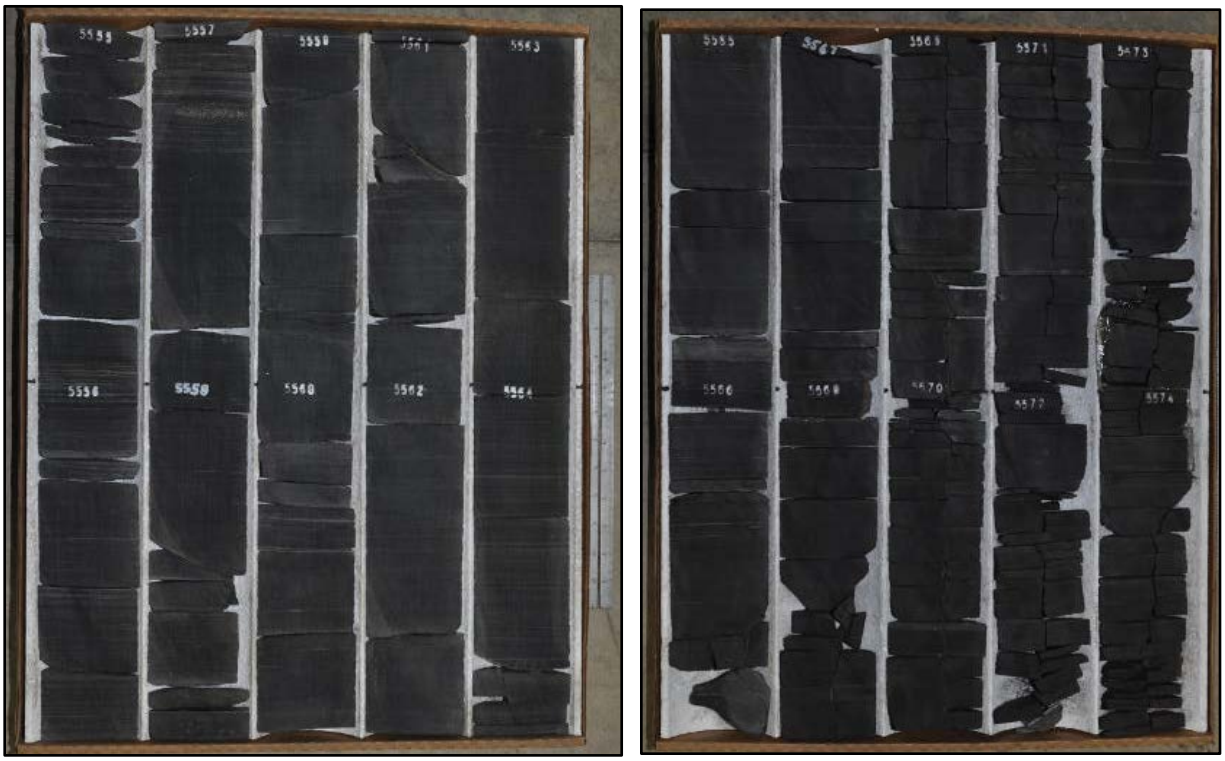

Figure 3: Tippens 6HS core photographs, from 5555 to 5575 ft.

Figure 4: Tippens 6HS core photographs, from 5575 to 5595 ft.

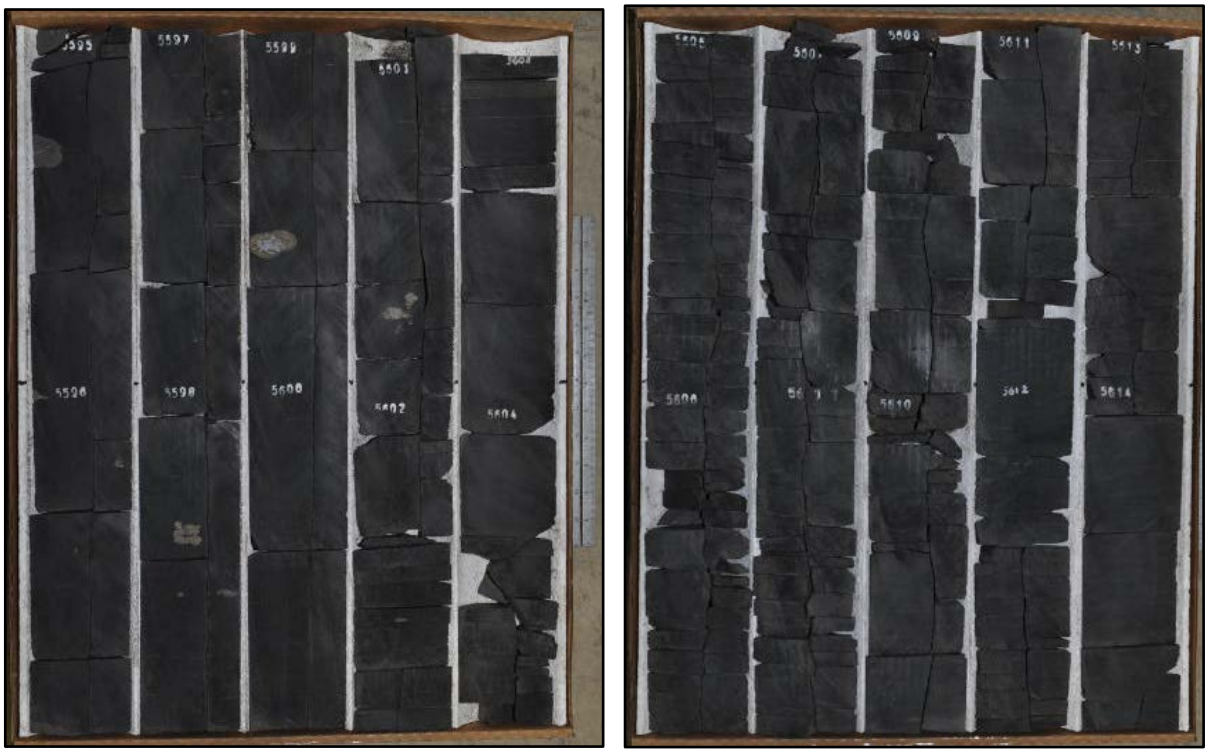

Figure 5: Tippens 6HS core photographs, from 5595 to 5615 ft.

Figure 6: Tippens 6HS core photographs, from 5615 to 5635 ft.

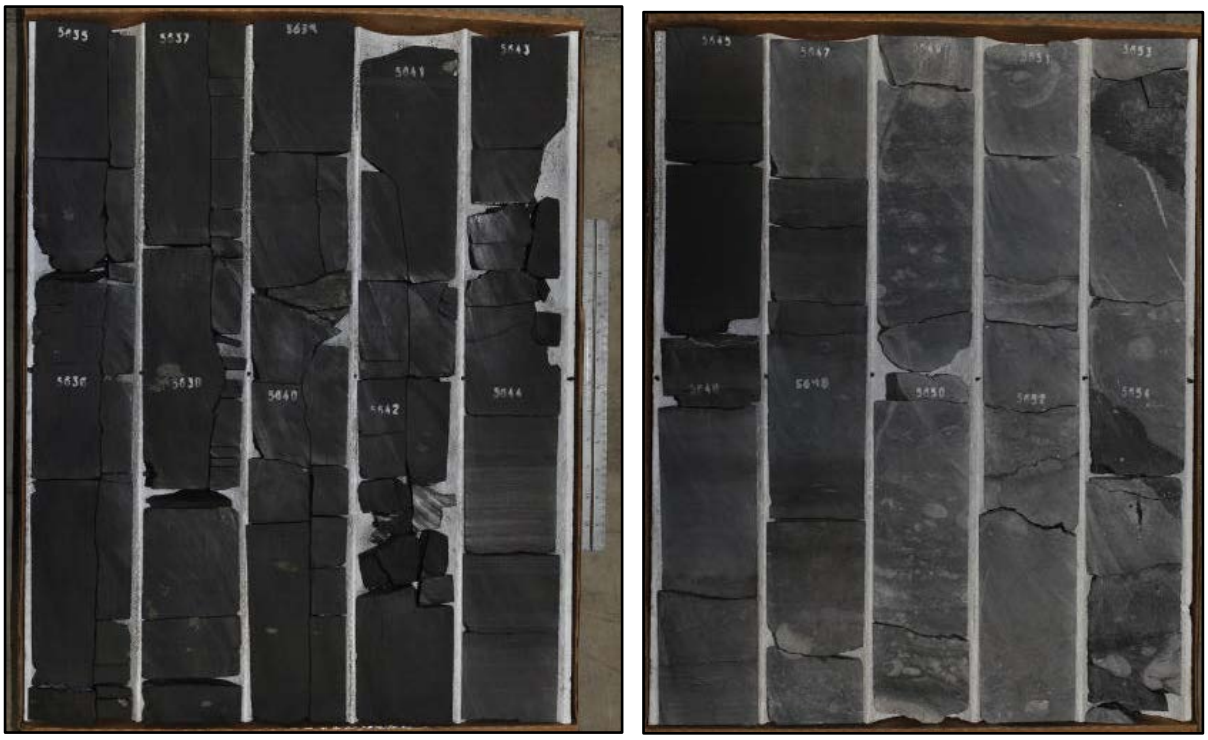

Figure 7: Tippens 6HS core photographs, from 5635 to 5655 ft.

Figure 8: Tippens 6HS core photographs, from 5655 to 5663 ft.

3. DATA ACQUISITION AND METHODOLOGY

The core was evaluated using computed tomography (CT) scanning and traditional core logging. CT scans were performed on the 2/3 slabbed cores to maximize the internal area of the core that could be visualized. Core logging was performed on the 1/3 slabbed cores due to the presence of a small channel that was cut from the center of each 2/3 slabbed core for mineralogical measurements prior to their arrival at NETL.

3.1 CORE LOGGING

Geophysical measurements of core thickness deviation, P-wave travel time, P-wave signal amplitude, magnetic susceptibility, and attenuated gamma counts can be obtained with a Geotek® Multi-Sensor Core Logging (MSCL) system on a competent core. For the 1/3 slabbed core that was scanned as part of this analysis the only geophysical measurement that could be accurately obtained was magnetic susceptibility. Additionally, the system was used to measure bulk elemental chemistry with a built-in, portable X-ray fluorescence (XRF) spectrometer. For a full description of the MSCL capabilities at NETL, please see Crandall et al. (2017). Only the XRF and magnetic susceptibility measurements are explained below.

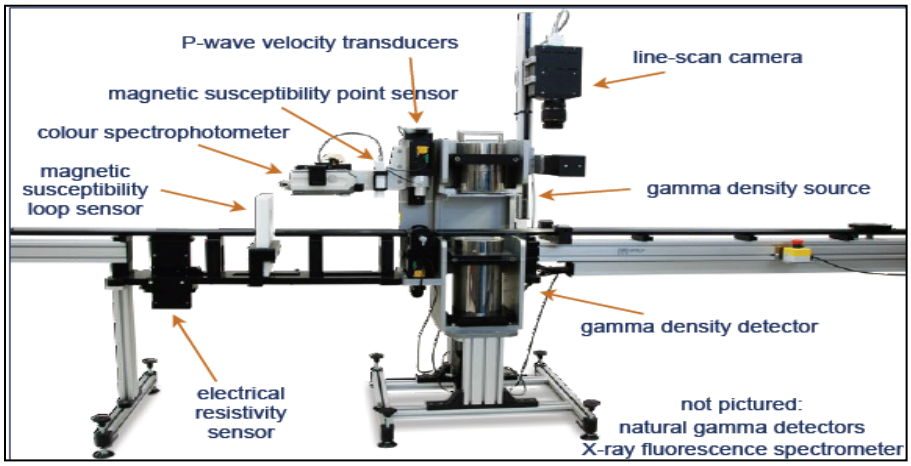

Figure 9: Representation of generalized MSCL with all attached instruments. From Geotek Ltd., Geotek Multi-Sensor Core Logger Flyer, Daventry, UK (2009).

3.1.1 Magnetic Susceptibility

Magnetic susceptibility is a measure of the degree of magnetization in the sample. The sample is passed through a ring apparatus with an oscillating magnetic field, where the interference to this field is proportional to the magnetism of the sample, and thus a relative measurement can be taken. The measurement unit used is dimensionless (abbreviated simply as SI units) and is based on the original calibration, which is done via stable iron oxides, and reference minerals which have known ranges of susceptibility (Table 1) (Geotek Ltd. Multi-Sensor Core Logger Manual, Version 05-10; Geotek, 2010).

Table 1: Magnetic susceptibility values for common minerals (modified from Geotek Ltd. Multi-Sensor Core Logger Manual, Version 05-10)

Mineral	X (*10^{-6}) SI
Water	9
Calcite	-7.5 to -39
Halite, Gypsum	-10 to -60
Illite, Montmorillonite	330 to 410
Pyrite	5 to 3,500
Hematite	500 to 40,000
Magnetite	1,000,000 to 5,700,000

3.1.2 X-ray Fluorescence Spectrometry

In addition to the geophysical measurements a portable handheld Innov-X® X-Ray Fluorescence Spectrometer was used to measure relative elemental abundances of aggregated "light elements" up to and including sodium, and also various heavy elements which were measured individually (Figure 5). Elemental abundances are reported relative to the total elemental composition, i.e. out of 100% weight.

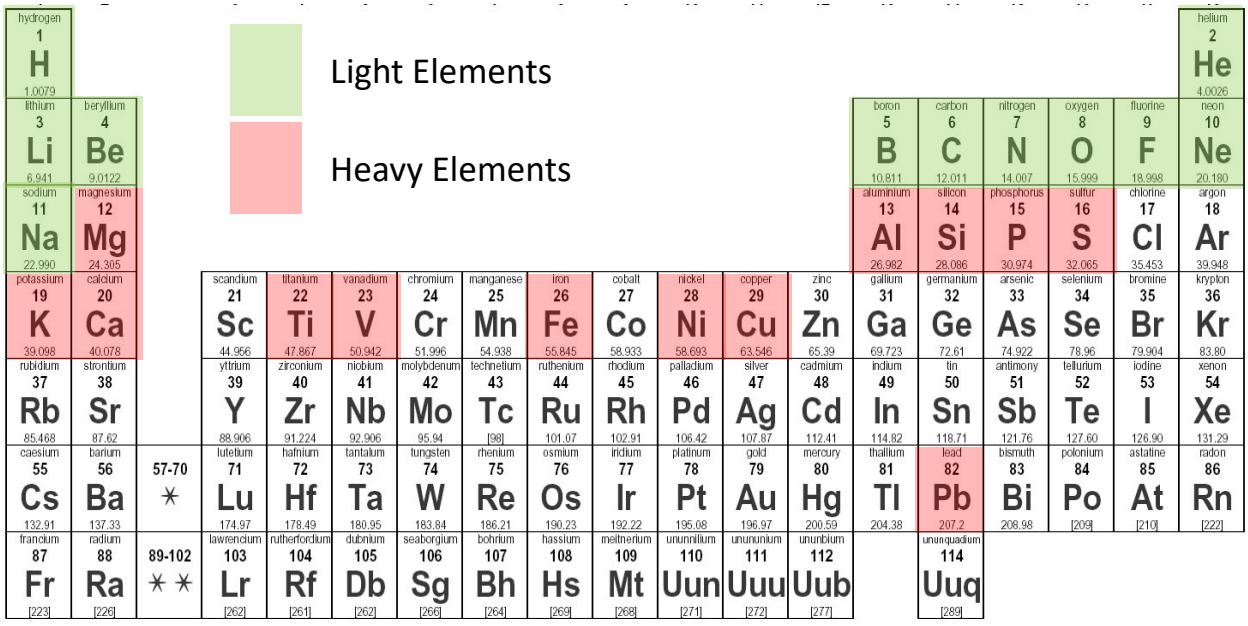

Figure 10: Periodic table showing elements measurable by the Innov-X® X-Ray Fluorescence Spectrometer.

The XRF spectrometer measures elemental abundances by subjecting the sample to X-ray photons. The high energy of the photons displaces inner orbital electrons in the respective elements. The vacancies in the lower orbitals cause outer orbital electrons to "fall" into lower orbits to satisfy the disturbed electron configuration. The substitution into lower orbitals causes a release of a secondary X-ray photon, which has an energy associated with a specific element. These relative and element specific energy emissions can then be used to determine bulk elemental composition.

3.2 MEDICAL CT SCANNING

Core scale CT scanning was done with a medical Toshiba® Aquilion TSX-101A/R medical Scanner as shown in Figure 11. The medical CT scanner generates images with a resolution in the millimeter range, with scans having voxel resolutions of 0.35 x 0.35 mm in the XY plane and 0.50 mm along the core axis. The scans were conducted at a voltage of 80 kV and at 200 mA. Subsequent processing and combining of stacks was performed to create three-dimensional (3D) volumetric representations of the cores and a two-dimensional (2D) cross-section through the middle of the core samples using ImageJ (Rasband, 2016). The variation in greyscale values observed in the CT images indicates changes in the CT number obtained from the CT scans, which is directly proportional to changes in the attenuation and density of the scanned rock. Darker regions are less dense. As can be seen in Figures 12–19, filled fractures, open fractures, and changes in bedding structure can all be resolved via careful examination of the CT images. While the medical CT scanner was not used for detailed characterization in this study, it allowed for non-destructive bulk characterization of the core, and thus complimented the MSCL data on the resultant log.

Figure 11: Toshiba® Aquilion™ Multislice Helical Computed Tomography Scanner at the NETL used for core analysis.

3.3 DATA COMPILATION

Strater® by Golden Software® was used to compile the MSCL and medical CT data into a series of geophysical logs. This data can be accessed from NETL's Energy Data eXchange (EDX) online system using the following link: https://edx.netl.doe.gov/dataset/tippens-6hs-well.

4. RESULTS

Processed 2D slices of the medical CT scans through the cores are shown first, followed by the XRF and magnetic susceptibility measurements of the core from the MSCL.

4.1 MEDICAL CT SCANS

As was discussed previously, the variation in greyscale values observed in the medical CT images indicates changes in the CT number obtained, which is directly proportional to changes in the attenuation and density of the scanned rock (i.e. darker regions are less dense).

Core was scanned in 3 ft or smaller sections due to the limitation of how many images could be generated for each scan. In highly-fractured core, sections in excess of 3 ft were often scanned. Detailed information in log books and photographs of cores were used to merge multiple scans of cores when this occurred. In the following images, the reported depth (top and bottom) for each scanned sub-section of core is listed.

Interesting features determined from visual analysis of the core include:

- Calcareous sections at 5565.9, 5586 and 5644.3 ft
- Large pyrite nodule at 5576.2 ft
- Cross-cutting calcite vein at 5577.6 ft
- A wavy lamination with marine fossils and pyrite replacement at 5586 ft
- Pyrite concretions and veins at 5588.5 ft
- Distorted beds and storm deposits at 5593.6 ft
- Calcite veins at 5594.6 ft
- Below 5646 ft the unit is more calcareous with less organic content
- Several beds are bioturbated and contain marine fossils
- Calcite clasts and veining that crosscuts bedding with cavities and vugs appearing at a depth of 5658.6 ft

Many of these features can readily be seen in the following images.

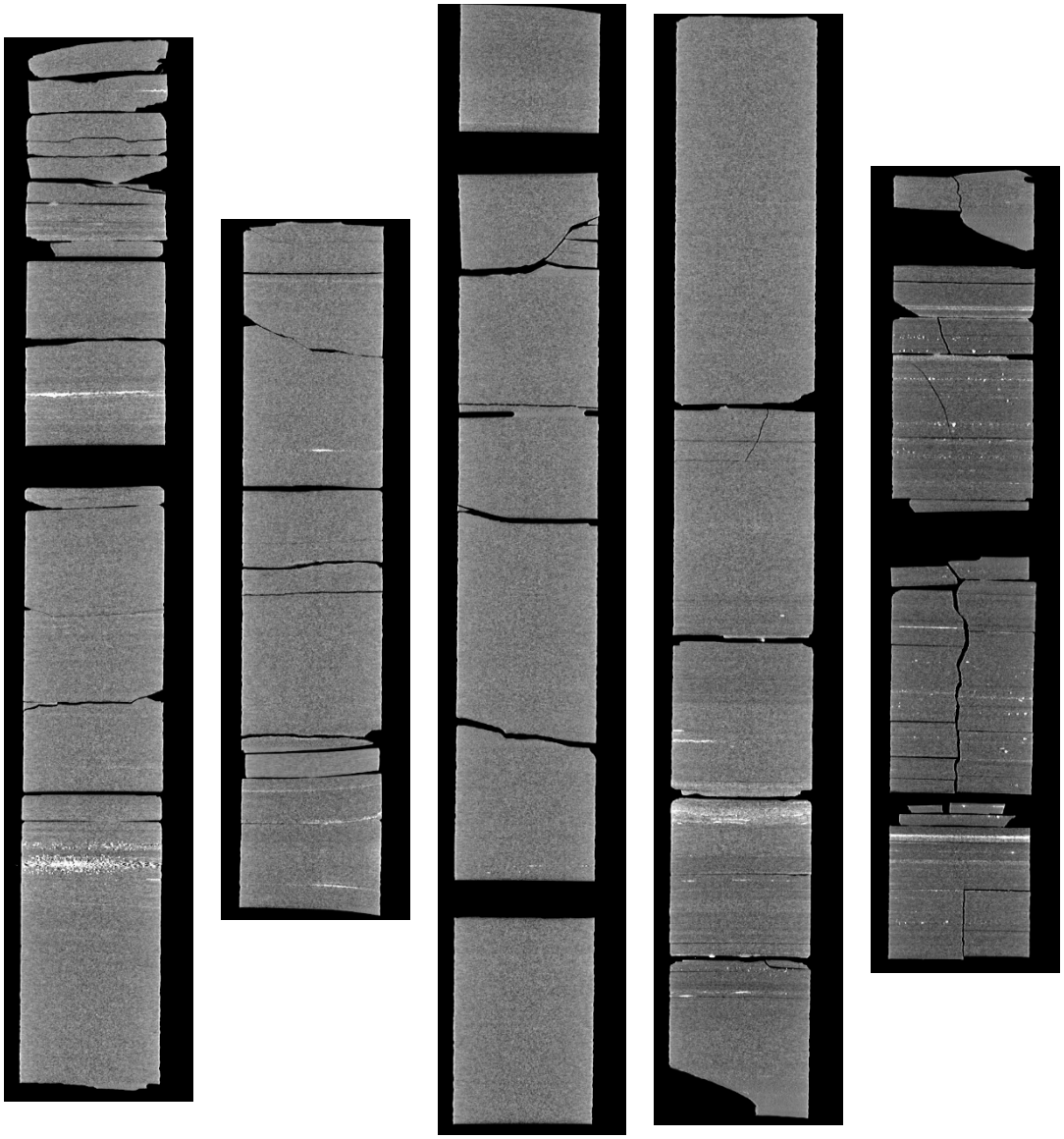

5555.0 – 5557.84 **5557.84 – 5560.71** **5560.71 – 5564.75** **5564.75 – 5566.73** **5566.73 – 5569.71**

Figure 12: Tippens 6HS, medical CT scans from 5555.0 to 5569.7 ft.

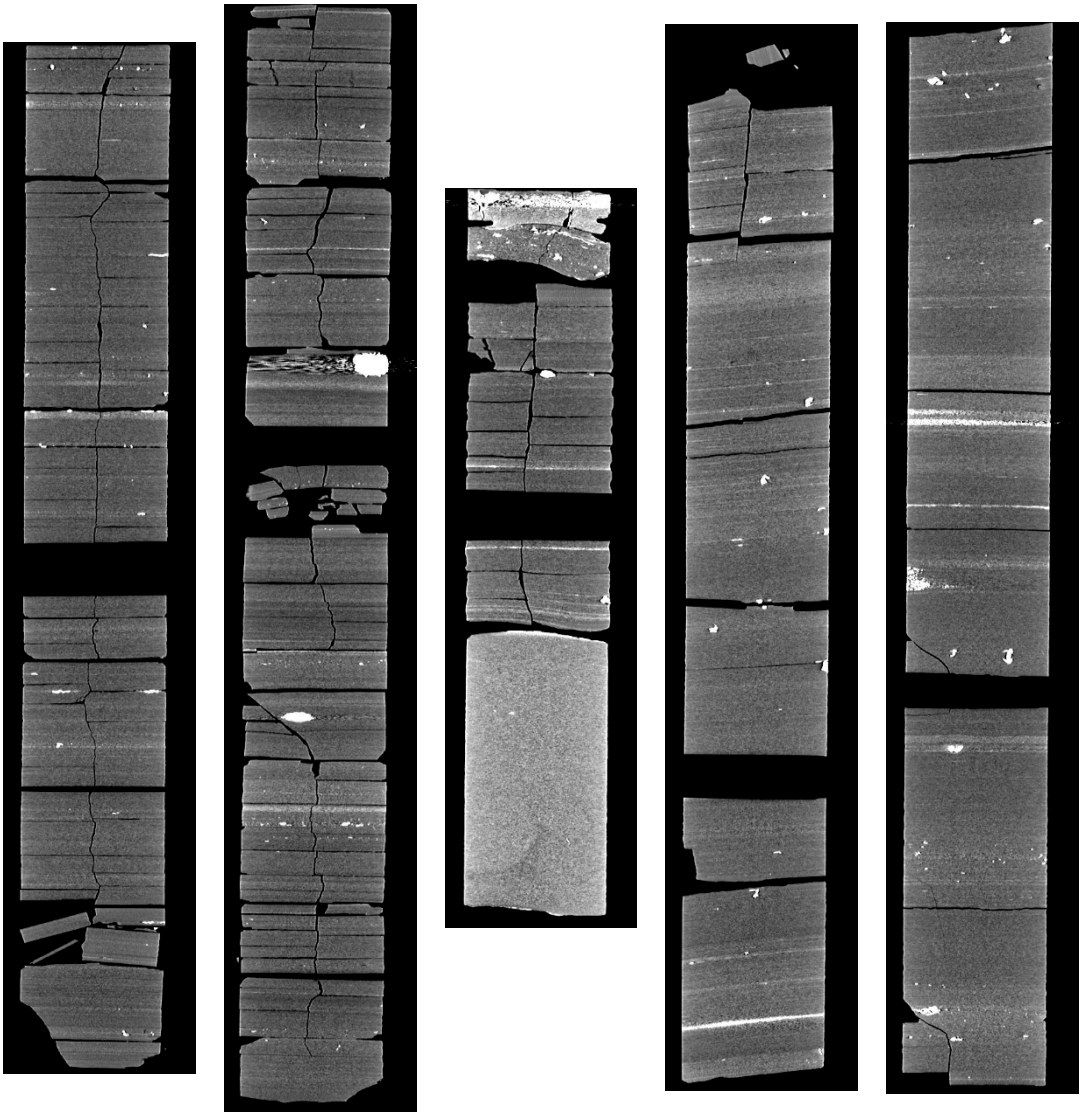

5569.71 – 5572.40 **5572.40 – 5575.35** **5575.35– 5578.18** **5578.18 – 5579.90** **5579.90 – 5583.72**

Figure 13: Tippens 6HS, medical CT scans from 5569.7 to 5583.7 ft.

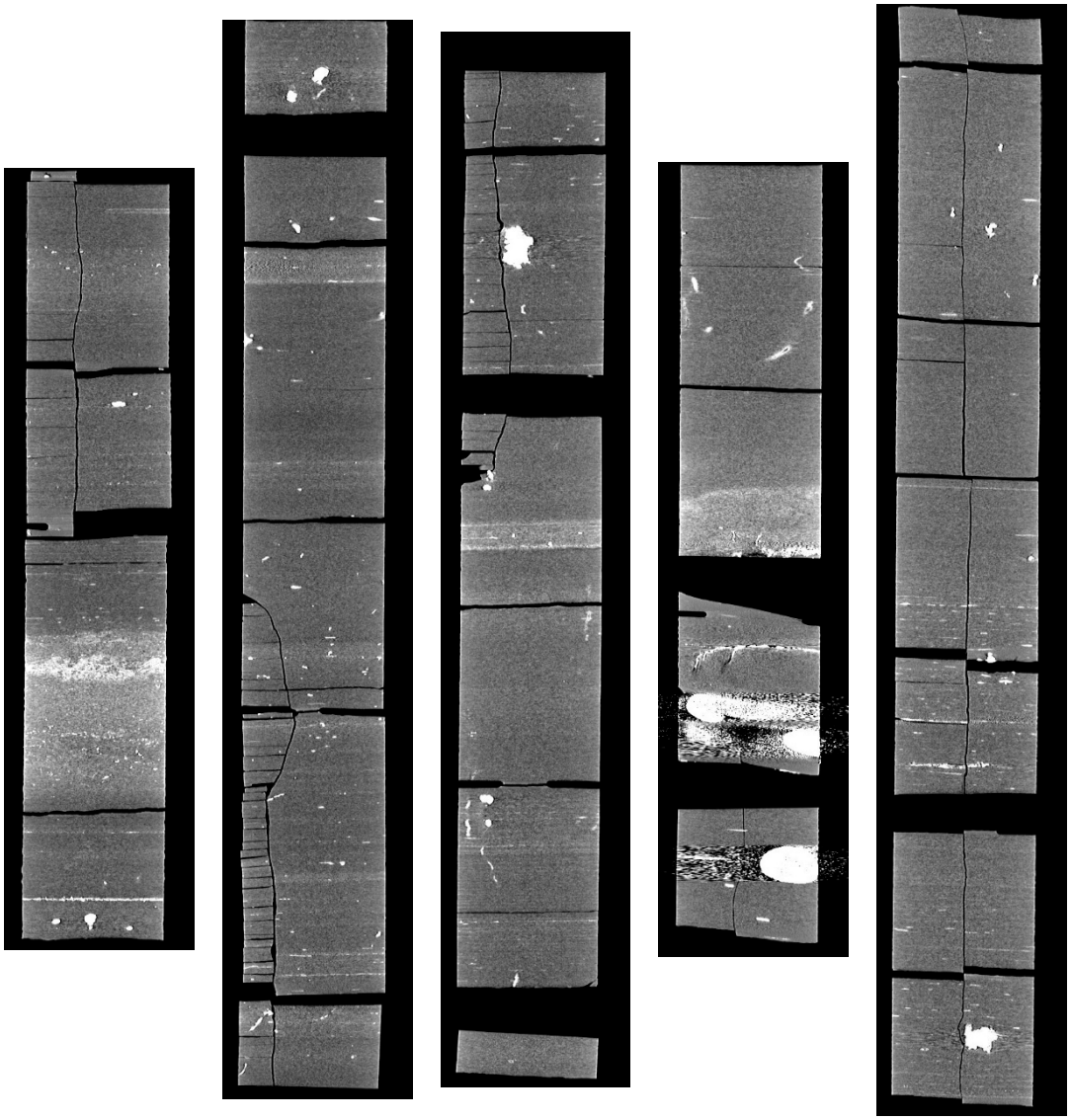

5583.72 – 5586.78 **5586.78 – 5589.71** **5589.71 – 5592.48** **5592.48 – 5595.90** **5595.90 – 5598.45**

Figure 14: Tippens 6HS, medical CT scans from 5583.7 to 5598.45 ft.

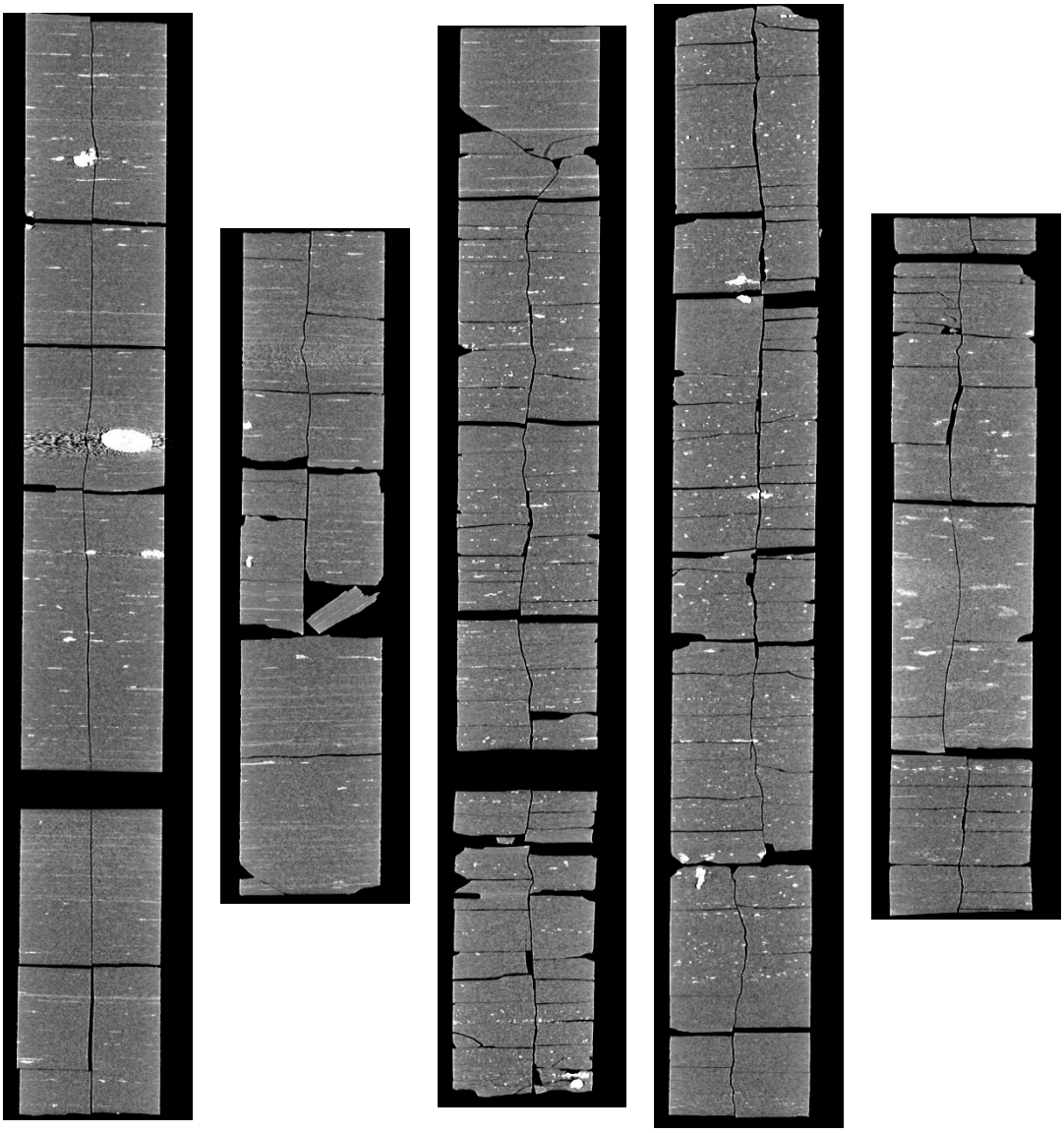

5598.45 – 5601.41 **5601.41 – 5604.15** **5604.15 – 5607.0** **5607.0 – 5610.0** **5610.0 – 5613.0**

Figure 15: Tippens 6HS, medical CT scans from 5598.45 to 5613.0 ft.

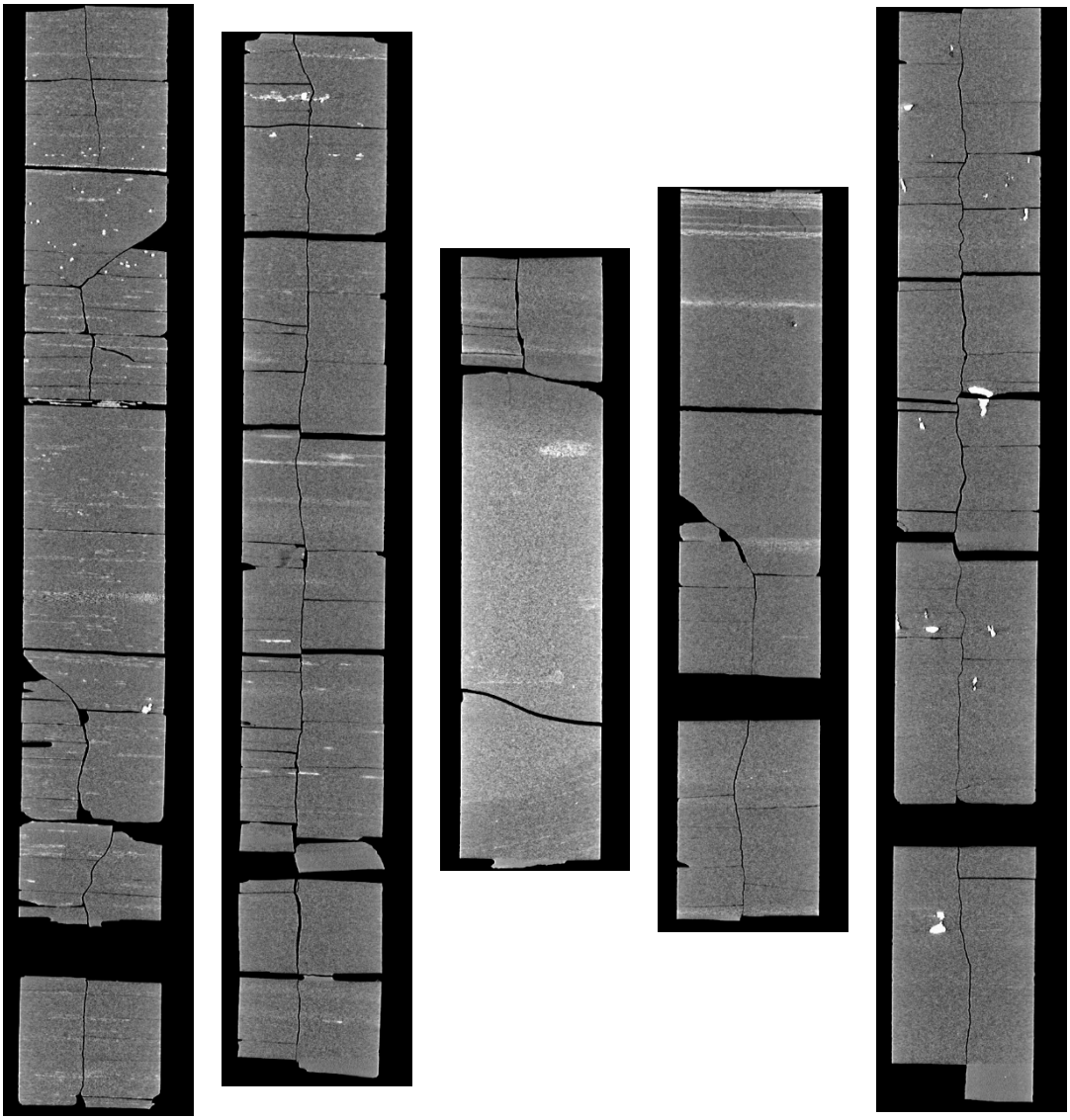

5613 – 5616 **5616 – 5619.38** **5619.38 – 5621.47** **5621.47 – 5624.43** **5624.43 – 5627.25**

Figure 16: Tippens 6HS, medical CT scans from 5613.0 to 5627.25 ft.

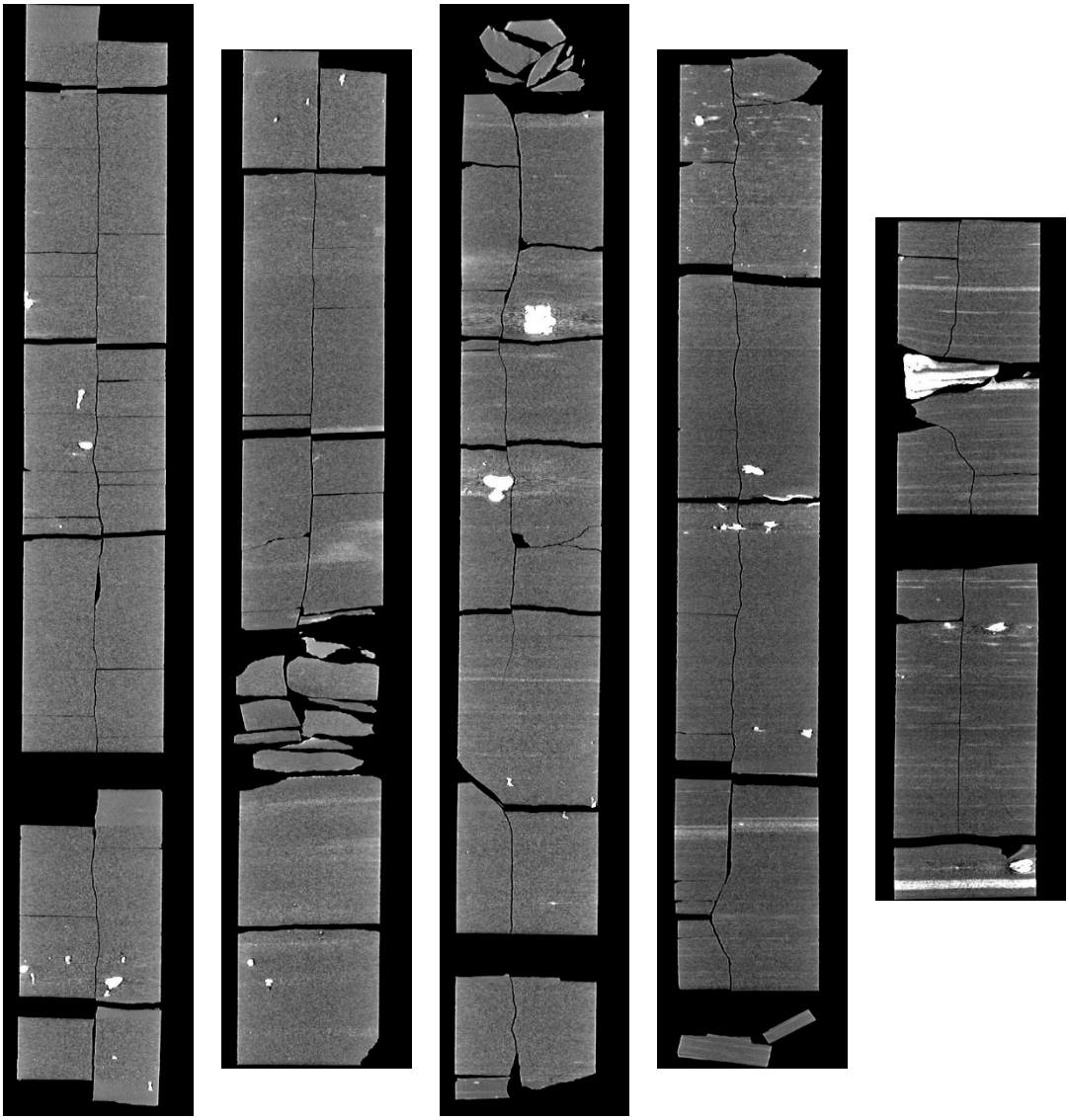

5627.25 – 5629.17 **5629.17 – 5633.0** **5633.0 – 5635.75** **5635.75 – 5638.40** **5638.40 – 5641.30**

Figure 17: Tippens 6HS, medical CT scans from 5627.25 to 5641.30 ft.

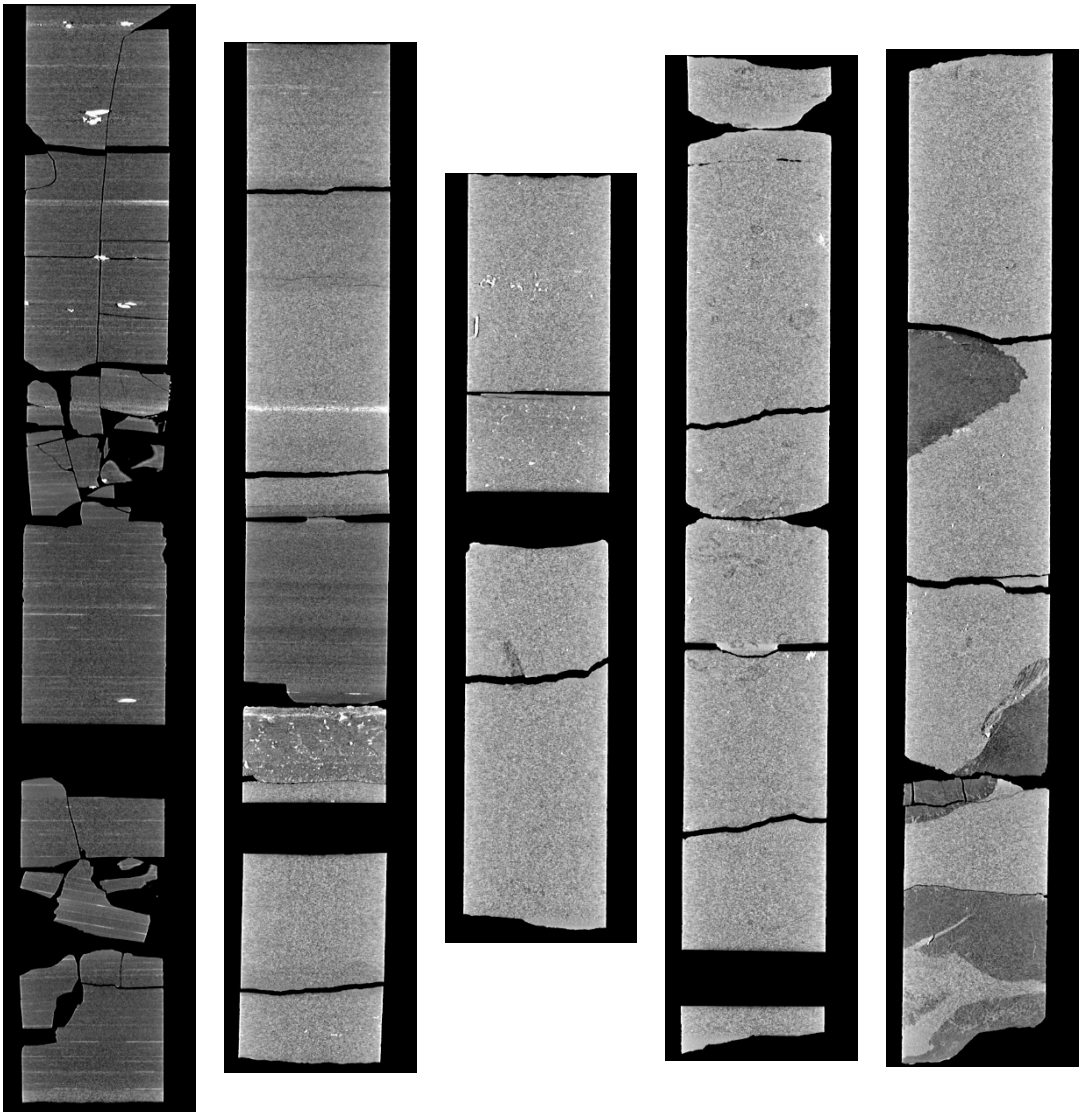

5641.30 – 5644.10 **5644.10 – 5646.80** **5646.80 – 5649.81** **5649.81 – 5652.44** **5652.44 – 5655.02**

Figure 18: Tippens 6HS, medical CT scans from 5641.30 to 5655.02 ft.

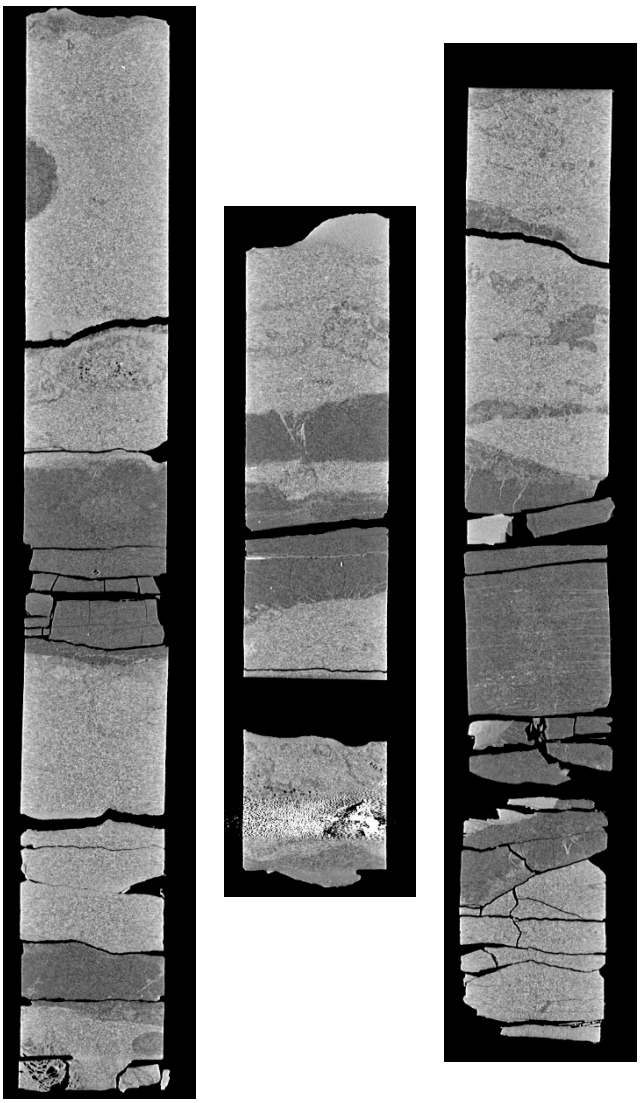

5655.02 – 5657.72 **5657.72 – 5660.56** **5660.56 - 5563**

Figure 19: Tippens 6HS, medical CT scans from 5655.02 to 5563 ft.

4.2 ADDITIONAL CT DATA

Additional CT data can be accessed from NETL's EDX online system using the following link: https://edx.netl.doe.gov/dataset/tippens-6hs-well. The original CT data is available as 16-bit tif stacks suitable for reading with ImageJ (Rasband, 2018) or other image analysis software. In addition, videos showing the variation along the length of the cross-section images shown in the previous section are available for download and viewing. A single image from these videos is shown in Figure 20, where the distribution of high density minerals in a cross section of the core around a depth of 5567 ft is shown. Here, the red line through the XZ-plane image of the core shows the location of the XY-plane displayed above. The videos on

https://edx.netl.doe.gov/dataset/tippens-6hs-well show this XY variation along the entire length of the core.

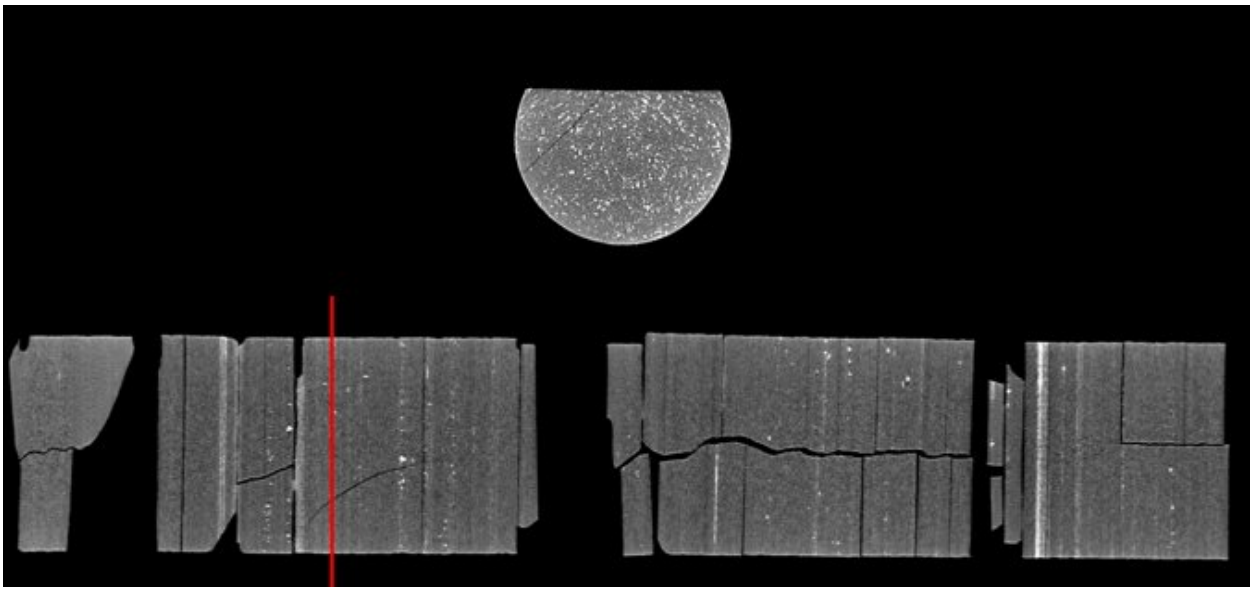

Figure 20: Single image from a video file available on EDX showing variation in the Tippens 6HS core from 5566.73 to 5569.71 ft. Image above shows the variation in composition within the matrix perpendicular to the core length.

4.3 COMPILED CORE LOGS

The compiled core logs were designed to be on single pages for rapid review of the combined data from the medical CT scans and MSCL readings. Features that can be derived from these combined analyses include determination of mineral locations, such as pyrite, from magnetic susceptibility and using the XRF to inform geochemical composition and mineral form. Examples include: Ca/Si provides information on relative carbonates versus silicates (i.e. clastic, including clays); Ca/Al gives carbonate versus clays and feldspar; and K/Al provides information on the abundance of illite and micas versus other clays. Fe/S is a proxy for oxidation state where reduced conditions would favor organic carbon. If reduced Fe is likely tied up in pyrite (Fe_2S) the ratio is high. If the ratio is >50% then there is "free" S or SO_3 in the system (e.g. other sulphides or sulphates). If oxidized Fe is in some form of iron oxide or hydroxide and not tied to S, the ratio is very low. There is no common Fe sulphate, so Fe should be either in sulphide or in oxide. Natural gamma is a proxy for organic carbon as well.

These are presented in the following images.

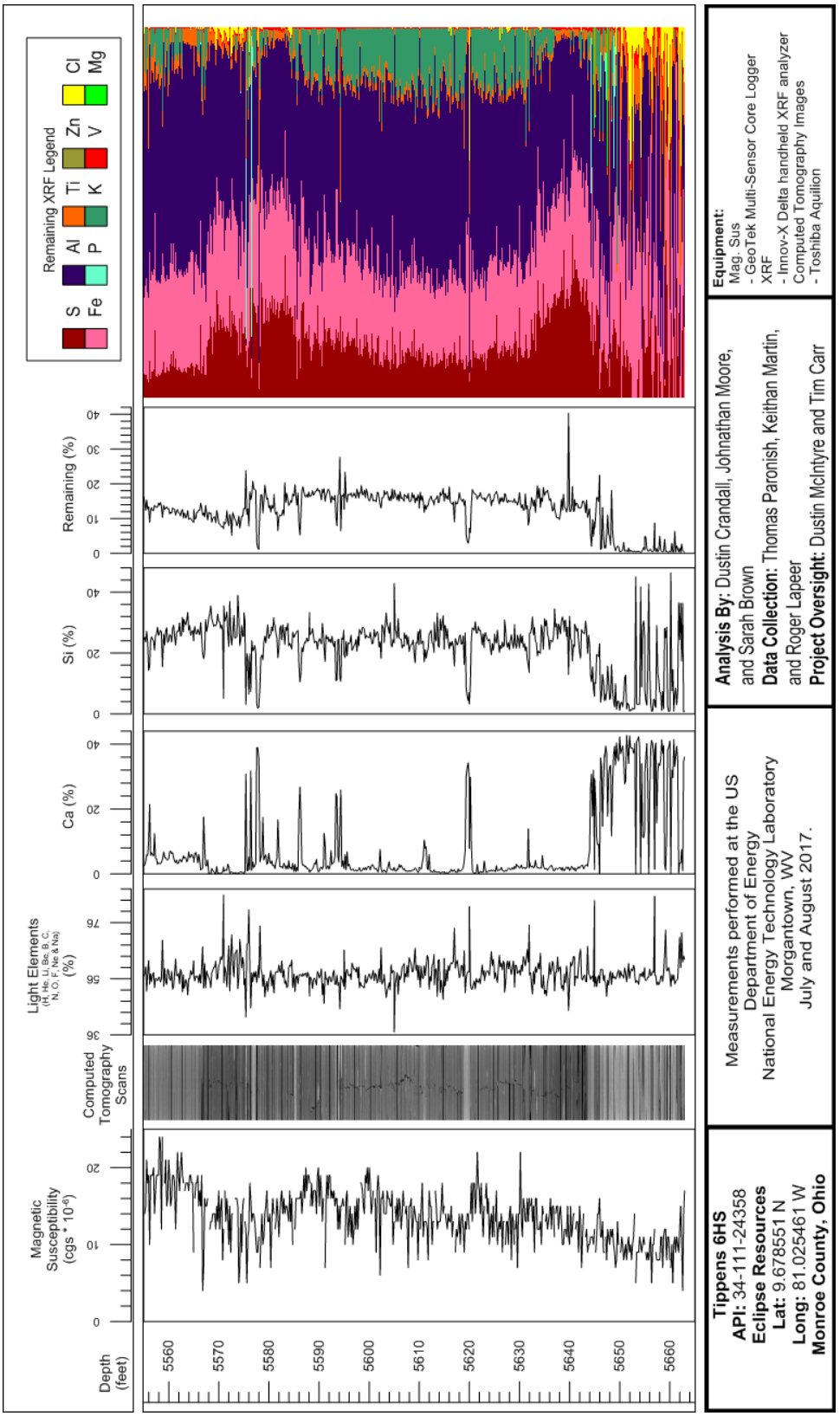

Figure 21: Combined core log for Tippens 6HS.

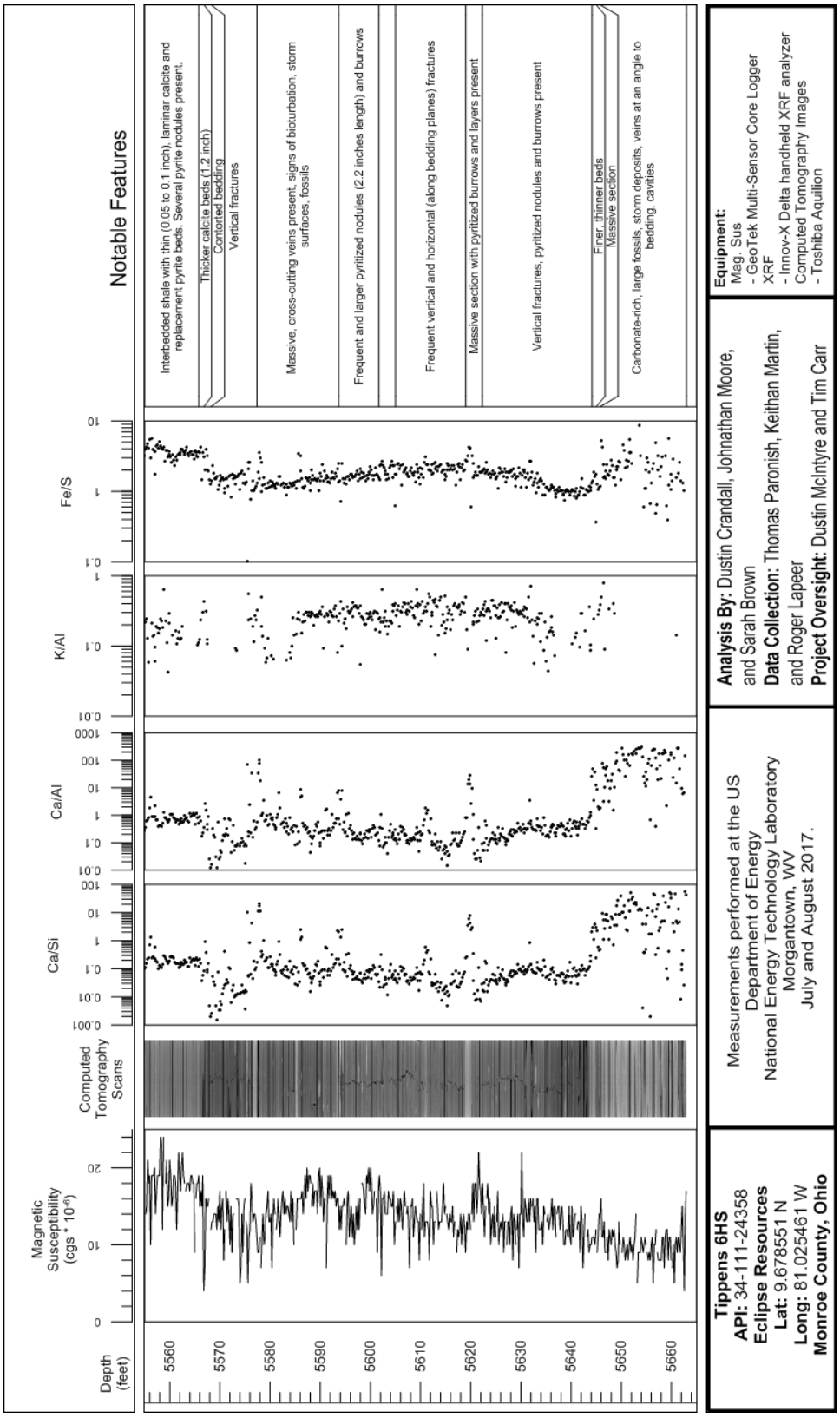

Figure 22: Core log with calculated elemental ratios and core description for Tippens 6HS.

5. DISCUSSION

The combination of the magnetic susceptibility, XRF, and CT analysis provides a unique look into the internal structure of the core and the macroscopic changes in lithology. These techniques are all non-destructive, rapid, and when performed in parallel give insight into the core features that is beyond what one individual technique can provide. Data sets presented here can be used to identify zones of interest within larger cores for detailed analysis and quantification.

6. REFERENCES

Crandall, D.; Moore, J.; Rodriguez, R.; Gill, M.; Soeder, D.; McIntyre, D.; Brown, S. *Characterization of Martinsburg Formation using Computed Tomography and Geophysical Logging Techniques*; NETL-TRS-4-2017; NETL Technical Report Series; U.S. Department of Energy, National Energy Technology Laboratory: Morgantown, WV, 2017; p 68.

Energy Information Administration, shapefiles from https://www.eia.gov/maps/maps.htm#shaleplay (accessed January 2018).

Geotek Ltd. Geotek Multi-Sensor Core Logger Flyer, Daventry, UK, 2009. http://www.geotek.co.uk/sites/default/files/MSCLOverview.pdf

Geotek Ltd. Multi-Sensor Core Logger Manual; Version 05-10; Published by Geotek, 3 Faraday Close, Daventry, Northamptonshire NN11 8RD, 2010. info@geotek.co.uk, www.geotek.co.uk

Rasband, W. S.; ImageJ. U.S. National Institutes of Health: Bethesda, MD, 1997–2016, http://imagej.nih.gov/ij/ (accessed 2018).

Sean Plasynski
Executive Director
Technology Development & Integration Center
National Energy Technology Laboratory
U.S. Department of Energy

Jared Ciferno
Associate Director
Oil and Gas
Technology Development & Integration Center
National Energy Technology Laboratory
U.S. Department of Energy

Elena Melchert
Director
Division of Upstream Oil and Gas Research
U.S. Department of Energy

David Alman
Executive Director, Acting
Research & Innovation Center
National Energy Technology Laboratory
U.S. Department of Energy

NETL Technical Report Series